

# UC Santa Barbara

## UC Santa Barbara Previously Published Works

### Title

A new ion sensing deep atomic force microscope

### Permalink

<https://escholarship.org/uc/item/4xt2m11z>

### Journal

Review of Scientific Instruments, 85(8)

### ISSN

0034-6748

### Authors

Drake, Barney  
Randall, Connor  
Bridges, Daniel  
[et al.](#)

### Publication Date

2014-08-01

### DOI

10.1063/1.4893640

Peer reviewed

## A new ion sensing deep atomic force microscope

Barney Drake, Connor Randall, Daniel Bridges, and Paul K. Hansma  
*Department of Physics, University of California, Santa Barbara, California 93106, USA*

(Received 18 June 2014; accepted 10 August 2014; published online 25 August 2014)

Here we describe a new deep atomic force microscope (AFM) capable of ion sensing. A novel probe assembly incorporates a micropipette that can be used both for sensing ion currents and as the tip for AFM imaging. The key advance of this instrument over previous ion sensing AFMs is that it uses conventional micropipettes in a novel suspension system. This paper focuses on sensing the ion current passively while using force feedback for the operation of the AFM in contact mode. Two images are obtained simultaneously: (1) an AFM topography image and (2) an ion current image. As an example, two images of a MEMS device with a microchannel show peaks in the ion current as the pipette tip goes over the edges of the channel. This ion sensing AFM can also be used in other modes including tapping mode with force feedback as well as in non-contact mode by utilizing the ion current for feedback, as in scanning ion conductance microscopy. The instrument is gentle enough to be used on some biological samples such as plant leaves. © 2014 AIP Publishing LLC. [<http://dx.doi.org/10.1063/1.4893640>]

### I. INTRODUCTION

Atomic Force Microscopy (AFM) has grown since its invention (Binnig *et al.*, 1986) to include a wide range of capabilities including the capability of using force control during topographic imaging while simultaneously measuring other parameters (Eaton *et al.*, 2010). Scanning Ion Conductance Microscopy (SICM) (Hansma *et al.*, 1989) uses ion currents to control imaging of topography. Its ability to image in a non-contact mode has resulted in publications growing exponentially (Chen *et al.*, 2012) in large part due to the intellectual leadership of Yuri Korchev and his collaborators (Novak *et al.*, 2009; Zhukov *et al.*, 2012). In this paper, we describe a novel deep AFM with ion sensing capabilities, utilizing aspects of both SICM and AFM operation.

The history of ion sensing AFM with micropipettes began with a modification of a SICM design. A microfabricated probe incorporating a tip integral to a flexible silicon membrane (Figure 1(a)) (Prater *et al.*, 1991) was developed. The probe is mounted as an end cap to a 1.5 mm glass capillary tube and has a typical minimum pore opening of 250 nm. The increased mechanical robustness and high resonant frequency of the probe allowed the scan rates to be increased by up to 50 times higher than when using glass micropipettes. This design did provide a compliant probe but did not incorporate a feedback loop from the probe deflection. The feedback controlled only the ion current. Nevertheless, we have included it in this history because it concluded: “Finally, since the probe tip is mounted on a flexible membrane, the SICM, or one of these techniques mentioned above, could be combined with force microscopy by measuring the deflection of the membrane as the tip is scanned over a surface.”

The first instrument to actually control probe deflection, while measuring ion current, was based on a bent micropipette (Figure 1(b)) (Proksch *et al.*, 1996). The deflection of the micropipette was monitored using a standard beam bounce technique. The instrument could be operated in either

contact or tapping mode and simultaneously recorded both height (topography) and ion current images. In tapping mode, the bent micropipette was oscillated at its resonant frequency, typically between 50 and 100 kHz, at a free oscillation amplitude of approximately 10 nm rms. A Nuclepore polycarbonate membrane (Millipore), with 200 nm pores, was imaged both in contact and tapping mode. The tapping mode images showed significantly higher resolution, both in the height and ion current images, than the contact mode images due to reduced lateral forces between the tip and sample. The main problem was that it required special bent micropipettes. The main advantage was that it could image a membrane in AFM mode while simultaneously revealing pores that went all the way through the membrane. This was crucial for revealing the pores that enable the nacre of abalone shells to form (Schäffer *et al.*, 1997). Using AFM, SEM, and TEM, demineralized interlamellar sheets in abalone nacre were found to have holes, 5–50 nm in diameter, with an average spacing of about 50 nm. The ion sensing AFM images, over an area of about  $8 \times 8 \mu\text{m}$ , showed the holes to actually be pores through the membrane. This was instrumental in determining the nacre growth mechanism to be mineral bridge formation. The resolution of the ion conductance images were just able to reveal what appear to be individual pores and showed a distribution of 10–50 nS.

A seemingly logical next step in the development in combined AFM/SICM instruments was to use modern nanofabrication techniques to micro-machine a fluid channel into a silicon cantilever (Figure 1(c)). Our first attempt, in 1999, by Ami Chand, produced a few devices, but numerous problems, including very low yields and clogging of the tip opening, prevented obtaining publishable images. Though this general approach seems destined to succeed eventually, it has been difficult not only for our group, but other groups that have tried. We are unaware of any published images from this approach to date for AFM/SICM use. However, this approach has been wonderfully successful in the combined application of microfluidics and AFM, in the area of liquid dispensing and

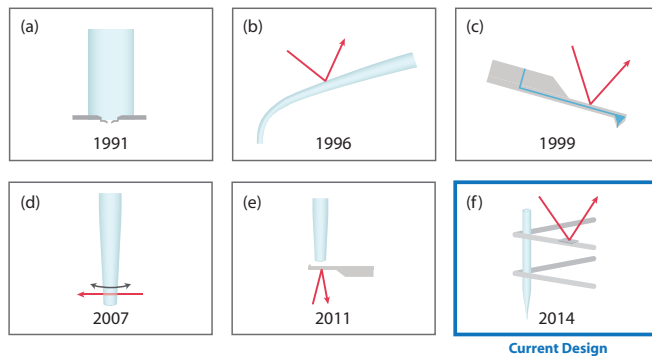


FIG. 1. The history of ion sensing AFM with pipettes. (a) A micromachined membrane is affixed to a glass pipette. (b) A curved pipette is used as the optical lever. (c) A micromachined AFM probe with internal fluid channel. (d) A pipette which senses transverse forces. (e) An inverted AFM probe is used to measure the forces due to hydrostatic pressure applied to a pipette. (f) The AFM introduced in this paper with ion sensing featuring a pipette affixed to a dual flexure optical lever.

manipulation of single living cells under physiological conditions (Meister *et al.*, 2009; Guillaume-Gentil *et al.*, 2014). Called fluidFM (fluid force microscopy), this technique utilizes a microfluidic probe, mounted to a cantilever holder with a mating port for fluid control. The probe holder has both a fluid reservoir and an external connection to a pressure controller. The impressive initial work demonstrated both intracellular injection, by force controlled perforation (at approximately 3 nN), and the staining of live neuroblastoma cells, with just gentle contact (less than 1 nN), by spontaneous diffusion across the cell membrane. The advancements since the initial work have shown the growing applications to include spatial manipulation, adhesion, and injection of single living cells under physiological conditions.

The next successful approach was a SICM with an integrated shear-force distance control that provides ion current measurements independent of sample topography (Figure 1(d)) (Böcker *et al.*, 2007). In this creative design, a 1 mm diameter micro pipette is submerged over the entire pulled length, while an optical detection system, using air filled periscopes, measures the lateral vibrational amplitude of the pipette near the tip. A dither piezo drives the lateral motion of the pipette at a fixed frequency, typically between 10 and 70 kHz, over distances of a few nanometers. The amplitude of the lateral motion decreases, as shear forces increase, when the tip is brought close to the sample surface, approximately 10–50 nm away. This amplitude reduction is used for the Z feedback signal to generate a topographic image while the ion current is recorded simultaneously. The sample, placed in an electrolyte filled dish, is mounted on a x,y,z scanner, with maximum ranges of 200  $\mu\text{m}$ , 200  $\mu\text{m}$ , and 20  $\mu\text{m}$  respectively. A new imaging mode was also introduced which was based on a periodic modulation of pipette to sample spacing, combined with triggered sampling, which helped to reduce both sample and pipette damage while also improving image quality. Typical modulation frequencies were 70–300 Hz with amplitudes between 50 and 250 nm.

Finally, Pellegrino and collaborators used an AFM cantilever as the sample! (Figure 1(e)) (Pellegrino *et al.*, 2011). In this work, hydrostatic forces were measured at the tip aper-

ture by monitoring cantilever deflection. If the current decrease values were below 2%, typical for far-scanning SICM mode, no hydrostatic forces were detected, if the level of the electrolyte filling the pipette is equal to that determined by capillary tension. They also showed that using hydrostatic forces of approximately 60 pN, the resultant mechanical stimuli could guide neuronal growth cones. Though they were primarily concerned with measuring the weak hydrostatic forces in SICM, their geometry could be used as an ion-sensing AFM.

Here we present a new approach in which a conventional pipette is held in a novel, soft suspension (Figure 1(f)). A small mirror (for which we use a conventional cantilever) is glued to the suspension to provide optical lever force detection for AFM. The ion currents are sensed with a Ag/AgCl wire electrode in the pipette.

## II. APPARATUS

A Dimension 3100 AFM with a Nanoscope V controller was used in combination with a custom nPoint NPXY400Z100 piezo stage to achieve a large scan range for imaging biological samples. The control system was the same as recently described in this journal for Deep AFM (Barnard *et al.*, 2013). A Dimension 3100 head was modified in order to accept the custom fabricated ion sensing probes. The head unit was only used for optical detection, the “Z” section of the piezo tube was removed in order to allow for adequate space to install the custom probes. The piezo tube was not necessary for this application because the microscope was set up as a sample-scanning microscope with the NPoint stage. For future applications, an adapter could be fabricated to accommodate the probes for use with the Dimension head unit without additional modifications.

The ion sensing probes utilized a new Deep AFM probe design (Barnard *et al.*, 2013) that enables longer tips for imaging while increasing the torsional stiffness to prevent lateral motion. This was important for this application due to the long pipette affixed to the probe. A prototype design is shown in Figure 2. This design uses two rectangular cross section flexures with a reflective coating. Other prototypes use wire with varying diameters to achieve the stiffness for the given application. A reflective mirror was bonded to the wire to enable the use of the optical lever.

Commercial micropipettes, purchased from Five Photon, were used with a range of inner diameters from 1  $\mu\text{m}$  to

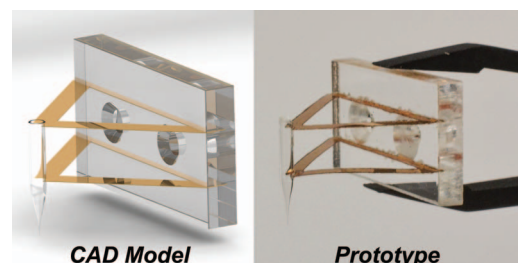


FIG. 2. Film flexure Deep AFM probe with ion current sensing capability. (Left) Rendering of a CAD model for the triangular film flexure probe. (Right) Prototype ion current sensing probe with gold coated flexures to reflect the laser back to the photodetector.

10  $\mu\text{m}$ . The micropipettes were cleaved in order to reduce the mass and prevent interference with the optical lever. The micropipette was then bonded to the flexure assembly with 2-ton Devcon epoxy. Before imaging, the micropipette was filled with saline solution and an internal filament provides capillary action to aid in filling without air bubbles.

Silver chloride ( $\text{Ag}/\text{AgCl}$ ) electrodes were used for the electrophysiological measurements. Electrical chloriding was achieved by using a solution of 1 M KCl with a current of approximately 10 mA for 5 min or until the wire was adequately plated by visual inspection. An electrode with a diameter of 0.25 mm was placed in the micropipette and a length of approximately 1 cm. A pellet electrode with a diameter of 2 mm was used in the sample holder which provided a more stable current over time. A 40 gauge insulated copper wire was soldered to the micropipette electrode and fixed to the probe holder. A fine wire was used in order to minimize the influence of the stiffness from the electrode connection. A schematic of the experimental setup is shown in Figure 3.

Contact mode imaging was straightforward. The challenge for tapping mode was the low resonant frequency of the assembly due to the large mass of the filled micropipette coupled to the soft cantilever. A resonant frequency of order 100 Hz was typical. To enable tapping mode, a much higher drive frequency is desirable. We overcame this challenge by implementing a magnetic drive based on the Lorentz Force that applied a force near the micropipette instead of the base. For the case of a current carrying straight wire the force is proportional to the current going through the wire and the magnetic field ( $F = I \times B$ ). A current was passed through the lower flexure support for the wire prototype. Permanent neodymium magnets were used to provide the magnetic field. A rendering of the experimental setup is shown in Figure 4.

Another imaging mode is based on traditional SICM but with force sensing capabilities. The ion current is used for feedback control for non-contact imaging. This mode could have applications for imaging soft biological samples and monitoring biological processes. An example could be imag-

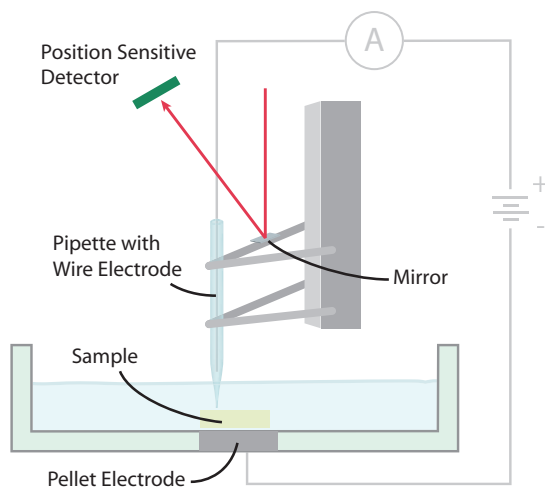


FIG. 3. A schematic overview of the ion sensing AFM probe in an instrument that can measure force by optical beam deflection as monitored with a Position Sensitive Detector and Ion currents between a pellet electrode and an electrode inside the pipette.

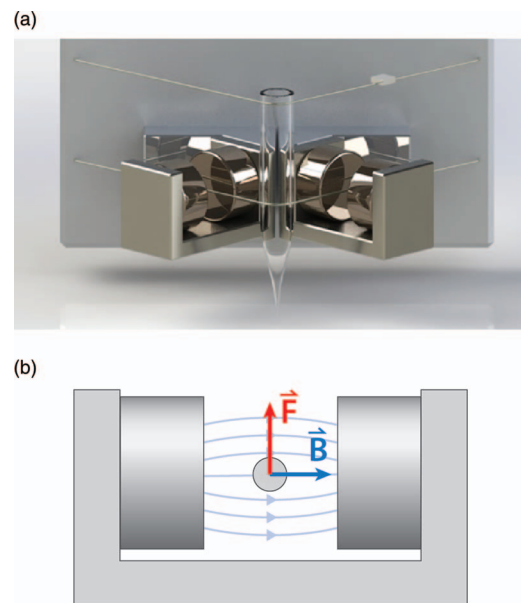


FIG. 4. Magnetic direct drive attachment capable of driving the probe tip at frequencies above the cantilever's natural frequency. (a) CAD rendering showing the placement of the permanent neodymium magnets. Current is passed through the bottom flexure wires to produce the magnetic field shown in (b). The induced force directly moves the pipette up and down allowing for complex drive modes such as tapping mode.

ing the action potential through a neural network by monitoring ion pulses along an axon. A traditional SICM that would only use current as feedback for the height could crash into the sample when it senses a spike in the ion current; however, with force sensing capabilities, the probe would gently tap the sample, similar to the tapping mode. An indication of a current spike would be displayed as a deflection in the probe detected through the optical lever. This would enable imaging soft biological samples as well as monitor any ion current spikes without damage to the probe.

### III. RESULTS

The first application involved imaging a MEMS device (Figure 5). The device was a microfluidic channel that consisted of a 50  $\mu\text{m}$  wide trench that was 10  $\mu\text{m}$  deep and a trench wall angle of 60°. The height profile shows the dimensions of the channel (minus the microfluidic probe diameter). The ion current is drastically different because of the high current that can be passed through the micropipette when the probe begins to overhang the trench. Once the micropipette reaches the bottom, the current drops again back to the same level on the top of the trench.

The next application was imaging a biological sample in contact mode. The sample imaged was the abaxial surface of a white clover (*Trifolium repens*) leaf showing two stomata. We investigated the opening of the stomata to demonstrate the ability of the instrument to image a delicate sample non-destructively. The stoma also provided a surface feature that showed differences in the height and ion current images, also demonstrating the usefulness of the combined imaging modes (Figure 6).



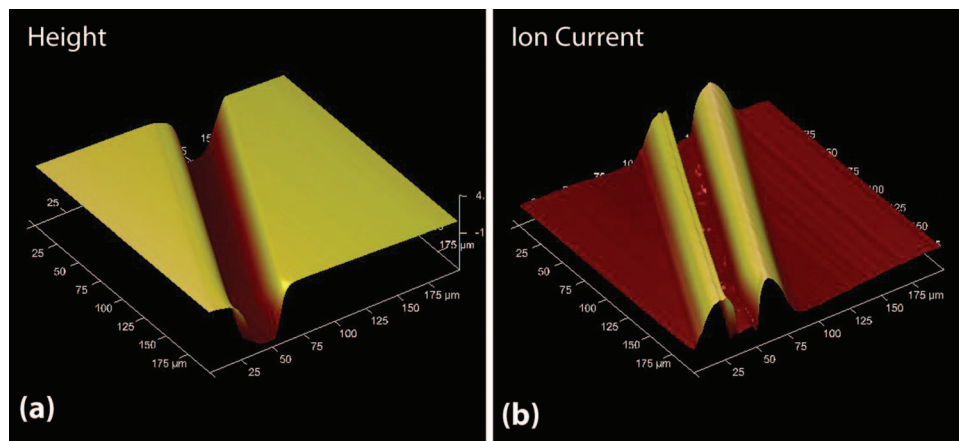


FIG. 5. A  $200\ \mu\text{m} \times 200\ \mu\text{m}$  image of a microfabricated fluid trench taken with a  $10\ \mu\text{m}$  ID pipette. (a) The resulting height image and (b) the ion current image. As the probe moves across the trench the pipette opening becomes less closed off by its proximity to the sample, causing the ion current to increase. Once the probe reaches the bottom of the trench the ion current returns to its baseline value until the probe starts to move up the opposite side.

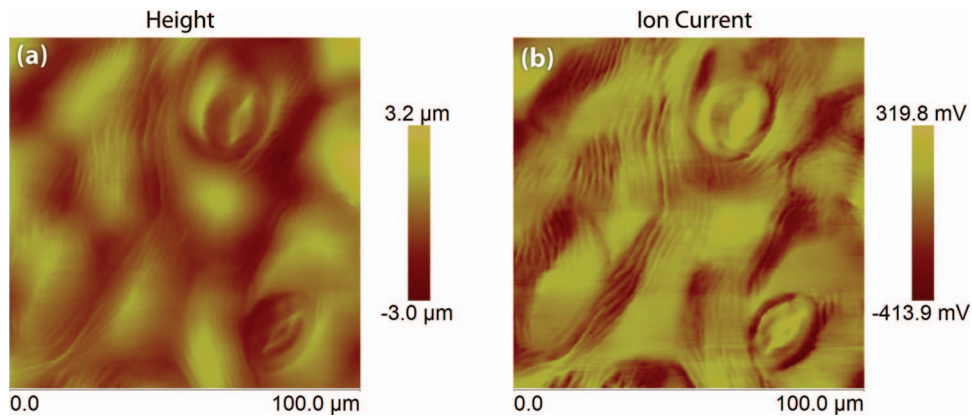


FIG. 6. Simultaneous height (left) and ion current (right) images of a white clover leaf (*Trifolium repens*), focusing on two stomata. The leaf was imaged in isotonic saline using a  $3\ \mu\text{m}$  ID pipette. The ion current image shows different features of the clover, specifically more gradients in the slope along the surface. The ridges traveling vertically in the image are more pronounced and there is a spike in the current near each of the stomatal openings.

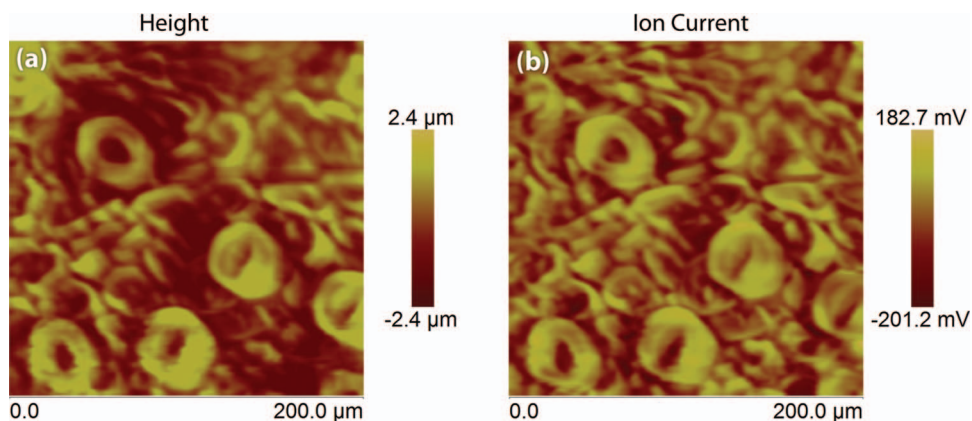


FIG. 7. Height (left) and ion current (right) images of an Indian Hawthorn leaf obtained in tapping mode. The tapping frequency was  $4.8\ \text{kHz}$ , much higher than the natural frequency of the probe assembly which is of the order of  $100\ \text{Hz}$ . This was achieved using the magnetic drive shown in Figure 4. The image was taken in isotonic saline with a  $10\ \mu\text{m}$  inner diameter micropipette.

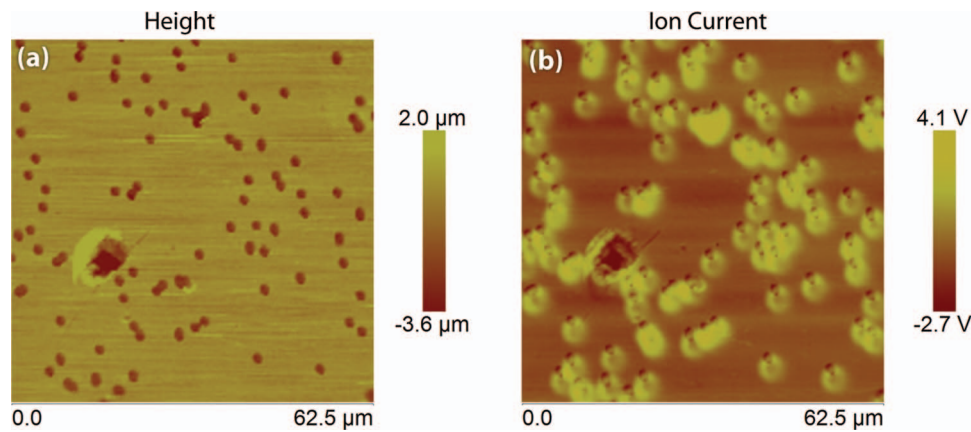


FIG. 8. Height (left) and ion current (right) images of a  $2\ \mu\text{m}$  polycarbonate Isopore™ membrane filter taken using a  $3\ \mu\text{m}$  ID pipette probe. Increased ion current is detected near the filter's holes, partially offset due to the tip geometry. Of particular note is the large defect on the left side of the images. The ion sensing image clearly shows that this defect does not penetrate the membrane, something not readily determined from the height image alone.

The next application was imaging another biological sample in tapping mode instead of contact mode. The sample imaged was the abaxial surface of an Indian Hawthorn leaf. This application tested the ability of the magnetic drive to enable tapping mode at much higher drive frequencies than the resonant frequency of the probe assembly without the magnetic drive. The image shown in Figure 7 displays both the height profile and the ion current in a scan of  $200\ \mu\text{m}$  obtained in tapping mode. The tapping frequency was  $4.8\ \text{kHz}$ , while the natural frequency of the probe assembly is of the order of  $100\ \text{Hz}$ . This demonstrates the capability of the magnetic drive to enable tapping at much higher frequencies, well above the natural frequency of the probe assembly.

The final application was imaging a  $2\ \mu\text{m}$  polycarbonate membrane filter (Millipore) in contact mode. The filter was attached to a lucite substrate with Devcon 2-ton epoxy. The lucite substrate was pre drilled with a  $230\ \mu\text{m}$  diameter hole that allowed access to the pellet electrode while also providing enough support to image the filter. This mounting arrangement restricted the ion current to flow only through the membrane filter, directly over the hole. A  $3\ \mu\text{m}$  ID pipette was positioned over the  $230\ \mu\text{m}$  hole during the imaging process. Figure 8 shows both height and ion current images. There is a large defect on the left side of both images that is essentially identical in both images. This suggests the defect does not penetrate through the filter. Also of interest is the difference in ion current flow through different pores in the filter. In the top center of the height image there is a cluster of four of five pores which appear to be connected. The corresponding area of the ion current image shows a much larger current than over individual pores.

#### IV. SUMMARY

This study introduced a novel deep AFM with ion sensing capabilities. A custom ion sensing probe was fabricated and adapted to a modified AFM head unit. The probe consisted of a micropipette fixed to dual flexures. This design creates a higher lateral torsional stiffness for the probe which is needed due to the relatively long length of a micropipette as compared

to tips on traditional AFM cantilevers. Different imaging techniques are possible with this design including contact mode, tapping mode, and non-contact SICM mode with force sensing capabilities. Four examples were presented as demonstrations of a few of the many potential applications of the new microscope.

#### ACKNOWLEDGMENTS

This research was supported by the National Institutes of Health (NIH) R01 GM065354 through the UCSB California Nanosystems Institute.

- Barnard, H., Drake, B., Randall, C., and Hansma, P. K., "Deep atomic force microscopy," *Rev. Sci. Instrum.* **84**, 123701 (2013).
- Binnig, G., Quate, C. F., and Gerber, C., "Atomic force microscope," *Phys. Rev. Lett.* **56**, 930 (1986).
- Böcker, M., Anczykowski, B., Wegener, J., and Schäffer, T. E., "Scanning ion conductance microscopy with distance-modulated shear force control," *Nanotechnology* **18**, 145505 (2007).
- Chen, C., Zhou, Y., and Baker, L. A., "Scanning ion conductance microscopy," *Annu. Rev. Anal. Chem.* **5**, 207–228 (2012).
- Eaton, P. J. and West, P., *Atomic Force Microscopy* (Oxford University Press, 2010), Vol. 10.
- Guillaume-Gentil, O., Potthoff, E., Ossola, D., Franz, C. M., Zambelli, T., and Vorholt, J. A., "Force-controlled manipulation of single cells: from AFM to FluidFM," *Trends Biotechnol.* **32**, 381–388 (2014).
- Hansma, P. K., Drake, B., Marti, O., Gould, S. A. C., and Prater, C. B., "The scanning ion-conductance microscope," *Science* **243**, 641–643 (1989).
- Meister, A., Gabi, M., Behr, P., Studer, P., Vörös, J., Niederman, P., Bittererli, J., Polesel-Maris, J., Liley, M., Heinzelmänn, H., and Zambelli, T. "FluidFM: combining atomic force microscopy and nanofluidics in a universal liquid delivery system for single cell applications and beyond," *Nano Lett.* **9**, 2501–2507 (2009).
- Novak, P., Li, C., Shevchuk, A. I., Stepanyan, R., Caldwell, M., Hughes, S., Smart, T. G., Gorelik, J., Ostanin, V. P., Lab, M. J., Moss, G. W. J., Frolenkov, G. I., Klenerman, D., and Korchev, Y. E., "Nanoscale live-cell imaging using hopping probe ion conductance microscopy," *Nat. Methods* **6**, 279–281 (2009).
- Pellegrino, M., Orsini, P., Pellegrini, M., Baschieri, P., Dinelli, F., Petracchi, D., Tognoni, E., and Ascoli, C., "Weak hydrostatic forces in far-scanning ion conductance microscopy used to guide neuronal growth cones," *Neurosci. Res.* **69**, 234–240 (2011).
- Prater, C. B., Hansma, P. K., Totonese, M., and Quate, C. F., "Improved scanning ion-conductance microscope using microfabricated probes," *Rev. Sci. Instrum.* **62**, 2634–2638 (1991).

- Proksch, R., Lal, R., Hansma, P. K., Morse, D. E., and Stucky, G. D., “Imaging the internal and external pore structure of membranes in fluid: Tapping Mode scanning ion conductance microscopy,” *Biophys. J.* **71**, 2155–2157 (1996).
- Schäffer, T. E., Ionescu-Zanetti, C., Proksch, R., Fritz, M., Walters, D. A., Almqvist, N., Zaremba, C. M., Belcher, A. M., Smith, B. L., Stucky, G. D., Morse, D. E., and Hansma, P. K., “Does abalone nacre form by heteroepitaxial nucleation or by growth through mineral bridges?,” *Chem. Mater.* **9**, 1731–1740 (1997).
- Zhukov, A., Richards, O., Ostanin, V., Korchev, Y. E., and Klenerman, D., “A hybrid scanning mode for fast scanning ion conductance microscopy (SICM) imaging,” *Ultramicroscopy* **121**, 1–7 (2012).